Hindawi
Journal of Chemistry
Volume 2017, Article ID 6215315, 7 pages
https://doi.org/10.1155/2017/6215315

Research Article

Density Functional Theory Investigation into the B and Ga Doped Clean and Water Covered γ-Alumina Surfaces

Lihong Cheng,[1] Tianliang Xu,[2] Wenkui Li,[1] Zhiqin Chen,[1] Jianping Ai,[1] Zehua Zhou,[1] and Jianwen Liu[3]

[1]*Key Laboratory of Surface Engineering of Jiangxi Province, Jiangxi Science and Technology Normal University, Nanchang, Jiangxi 330013, China*
[2]*Zhengzhou Institute of Finance and Economics, Zhengzhou, China*
[3]*National Supercomputing Center in Shenzhen, Shenzhen 518055, China*

Correspondence should be addressed to Lihong Cheng; chenglihong001@126.com and Jianwen Liu; liujw@nsccsz.gov.cn

Received 15 February 2017; Accepted 15 March 2017; Published 26 April 2017

Academic Editor: Tao Wang

The structures and energies of the B and Ga incorporated γ-alumina surface as well as the adsorption of water are investigated using dispersion corrected density functional theory. The results show that the substitution of surface Al atom by B atom is not so favored as Ga atom. The substitution reaction prefers to occur at the tricoordinated A(4) sites. However, the substitution reaction becomes less thermodynamically favored when more Al atoms are substituted by B and Ga atoms on the surface. Moreover, the substitution of bulk Al atoms is not so favored as the Al atoms by B and Ga on the surface. The γ-alumina surface is found to have stronger adsorption ability for water than the B and Ga incorporated surface. The total adsorption energy increases as water coverage increases, while the stepwise adsorption energy decreases. The studies show the coverage of water at 7.5 H_2O/nm^2 (five H_2O molecules per unit cell) can fully cover the active sites and the further water molecule could only be physically adsorbed on the surface.

1. Introduction

The γ-alumina is an important material in chemistry and materials science due to its widespread applications in chemical industry [1–3], ceramics, and semiconductors [4–7]. In order to improve the performance of the material, some heteroatoms were usually chosen to be incorporated into the γ-alumina bulk and surfaces [8, 9]. For example, the Fe atom was usually used to improve the catalytic performance of γ-alumina [10]. Wan et al. investigated the Fe_2O_3/Al_2O_3 catalyst from coprecipitated and spray-dried method with Mösbauer spectroscopy [11] and found the reduction of Fe_2O_3 to FeO. The substitution of surface Al^{3+} by Fe^{3+} in alumina with mixed $(Al_{1-x}Fe_x)_2O_3$ surface formation is also confirmed by transmission Mösbauer spectroscopy. Integral low-energy electron Mösbauer spectroscopy and Fe K-edge X-ray absorption near-edge structure characterization observed the formation of iron nanoclusters from the transformation of γ-$(Al_{1-x}Fe_x)_2O_3$ to α-$(Al_{1-x}Fe_x)_2O_3$ and the iron distribution on the surface layers and in the cores of grains [12–14]. This field also attracts the interests of theoretical researches. Feng et al. calculated the structures and energies of the Fe promoted γ-alumina surface [10] and found that the incorporation of Fe atom into the γ-alumina surface is possible, while it is thermodynamically not so favored for the Fe substitution for the bulk Al atoms. The adsorption of water on the γ-alumina surface is stronger than that on the Fe_2O_3 covered surface. In addition, the electronic structures also change after the substitution of the Al atoms by the Fe atoms on the surface. Except for the incorporation of Fe into the alumina surface, the B and Ga atoms, which are often used as the trivalent substitution ions for the zeolites [15, 16], are also used in experiments for the preparation of high performance catalysis and semiconductors [8, 9, 17–19]. Kibar et al. prepared nanostructured boron doped alumina catalyst support [20] and found that the morphology of the supports can be modified from cracked surface to nanosphere formation by the introduction of boron. Jansons

et al. introduced Ga into the alumina crystal and prepared a new complex luminescence band at about 5 eV [19]. The Ga-related luminescence can be observed under the excitation of X-rays up to 600 K. In order to know the energies as well as the structures of the B and Ga incorporated γ-alumina surface at molecular level, the present work investigated the thermodynamic and structure properties of the B and Ga incorporated γ-alumina surface using dispersion corrected periodic density functional theory. Since γ-alumina is usually prepared and used in atmospheres containing water, the adsorption of water on the B and Ga incorporated γ-alumina is also investigated and compared with the water adsorption on pure γ-alumina surface.

2. Computational Details

The dispersion-corrected periodic density functional as implemented in the Vienna ab initio Simulation Package (VASP) was used for the calculations [21–23]. The DFT-D3 method of Grimme was used to take into account the dispersive interactions as previous work reported that the dispersion correction seriously influences the relative stability order and adsorption energies [24–28]. The exchange and correlation energies were calculated by the generalized gradient approximation (GGA) formulation with the PBE functional [21]. The Kohn-Sham one-electron states were extended in accordance with plane-wave basis sets with a kinetic energy of 400 eV. The projector augmented wave (PAW) method was applied to describe the electron-ion interactions [29–31].

The Brillouin zone was sampled with $5 \times 5 \times 5$ and $3 \times 3 \times 1$ k-points meshes generated by the Monkhorst-Pack algorithm, for the $p(1 \times 1 \times 1)$ γ-alumina cell and $p(1 \times 1)$ γ-alumina (110) surface slab, respectively. The convergence criteria were set to be 10^{-4} eV for the SCF energy, 10^{-3} eV and 0.03 eV/Å for the total energy and the atomic forces, respectively.

The γ-alumina surface was described using the Digne's model [32], and (110) surface was taken into account. As shown in Figure 1, γ-alumina surface was modeled using a $p(1 \times 1)$ supercell with an eight-layer slab, which contains sixteen Al_2O_3 units. A vacuum with thickness of 15 Å was employed to separate each slab from interactions. The top four layers and the adsorbates were fully relaxed, and the bottom four layers were fixed in their bulk position during the structure optimization. In order to facilitate the discussions, the surface layer Al and O atoms are indexed with number. The coordination number of each Al atom was expressed by subscript. As has been described in many previous works [33, 34], the Al atoms in bulk γ-alumina are in tetrahedral and octahedron sites. After cleavage, the tetrahedral and octahedron Al atoms expose as the tricoordinated and tetra-coordinated Al, respectively, in the (110) surface. As shown in Figure 1, the $Al(4)_{3c}$ was in tetrahedral site in the bulk, and $Al(1)_{4c}$, $Al(2)_{4c}$, and $Al(3)_{4c}$ were in octahedral sites in the bulk. It could be observed from the top view that Al(1) and Al(2) atoms are in the same chemical environment.

For the substitution of surface Al^{3+} by X^{3+} (X = B and Ga) in reaction (1) the substitution energy is defined as $E_{sub} = nE[Al(OH)_3] + E[Al_{(4-n)}X_nO_6{}^*] - nE[X(OH)_3] - E[Al_4O_6{}^*]$, where $E[X(OH)_3]$ and $E[Al_4O_6{}^*]$ present the energies of the gas phase $X(OH)_3$ and the isolated oxide surfaces ($*$ presents the 2–8 layers alumina substrate), respectively. The positive substitution energy means substitution reaction is not thermodynamically favored.

$$n\mathrm{X(OH)_3} + \mathrm{Al_4O_6}^* \longrightarrow n\mathrm{Al(OH)_3} + \mathrm{Al_{(4-n)}X_nO_6}^*. \quad (1)$$

The adsorption energy of nH_2O (n = 1–6) on the oxide surface was defined as $E_{ads} = E[(H_2O)_n \cdot X_4O_6{}^*] - nE(H_2O) - E(X_4O_6{}^*)$, where $E[(H_2O)_n \cdot X_4O_6{}^*]$, $E(H_2O)$, and $E(X_4O_6{}^*)$ are the total energies of the minima structures of $X_4O_6{}^*$ (X = B, Al, Ga) surface with adsorbed water, gas phase water molecule, and clean $X_4O_6{}^*$ surface, respectively. Following this definition, a more negative value indicates stronger interaction between adsorbed species and the surface.

$$n\mathrm{H_2O} + \mathrm{X_4O_6}^* \longrightarrow (\mathrm{H_2O})_n\,\mathrm{X_4O_6}^*. \quad (2)$$

3. Results and Discussion

3.1. Substitution of Al by B and Ga on the Surface. Table 1 shows the substitution energies for the substitution of Al by B and Ga on the surface. As indicated by the calculated substitution energies, the substitution of surface Al by B atoms is not thermodynamically favored, since the calculated substitution energies are positive. The tricoordinated Al(4) is the most favored site for one B incorporation with the substitution energy of 1.31 eV. The tetracoordinated Al(1) and Al(3) sites are slightly difficult with the substitution energies of 1.81 and 2.29 eV, respectively.

For two Al atoms substituted by B atoms on the surface, which corresponds to 50% surface, Al were replaced by B; the Al(1,2) are the most favored, with the substitution energy of 3.22 eV, versus Al(1,2,3) for 75% surface Al substitution by B, with the substitution energy of 5.32 eV. The substitution energies positively increase to 7.82 eV as all surface Al atoms were substituted by B atoms.

Figure 2 shows the structures for the B and Ga substituted γ-alumina surface. The corresponding bond distances of the surface layer atoms before and after the substitution are given in Table 1. It is found that the surface Al–O bond distances are in the range of 170–186 pm on the γ-alumina surface. After the substitution of Al by B atoms, the Al–O bond distance almost remains the same. It should be noted that the B–O bond distances (137–167 pm) are much shorter than those of the Al–O bonds, since the radius of B atom is much shorter than that of Al [35]. In addition, the B atom prefers to be tricoordinated, for example, for B(1,2,3,4) in Figure 2, bond e is elongated to 255 pm and became broken.

Since the substitution energies for the substitution of Al by Ga are much less than those for B substitution, the Ga could be more easily incorporated into to the alumina surface than B. Particularly for the Ga(4) structure, the substitution energy is −0.06 eV, which indicates the substitution reaction at Al(4) site by Ga is thermodynamically favored. Similar to that of B substitution, the substitution energy increases as more Al atoms were replaced by Ga atoms, for example, the substitution energies are 0.11, 0.49, and 0.90 eV, respectively,

Table 1: Substitution energies (E_{sub}) and the M–O bonds distances (pm) of the surface layer atoms before and after substitution for B and Gain γ-alumina (110) surface.

Substituted sites	E_{sub} (eV)	M(1)–O, a–d[a]	M(2)–O, e–h[a]	M(3)–O, i–l[a]	M(4)–O, m–o[a]
γ-alumina		174, 185, 173, 182	185, 174, 173, 182	186, 186, 180, 170	180, 171, 171
B(1)	1.81	141, 225, 137, 145	183, 176, 172, 183	184, 187, 179, 169	181, 175, 171
B(3)	2.29	173, 185, 172, 182	185, 173, 172, 182	167, 167, 149, 138	181, 171, 171
B(4)	1.31	173, 183, 177, 185	183, 173, 177, 185	185, 185, 181, 171	149, 139, 139
B(1,2)	3.22	142, 232, 136, 145	232, 142, 136, 145	186, 186, 178, 169	188, 176, 176
B(2,3)	3.94	175, 182, 173, 184	227, 141, 137, 145	147, 218, 145, 136	181, 171, 176
B(2,4)	3.58	175, 191, 174, 183	166, 145, 146, 155	184, 185, 181, 170	147, 138, 142
B(3,4)	3.70	172, 182, 177, 185	182, 172, 177, 185	164, 164, 151, 139	150, 139, 139
B(1,2,3)	5.32	141, 235, 136, 145	235, 141, 136, 145	165, 165, 149, 138	188, 177, 177
B(1,2,4)	6.02	145, 188, 142, 151	188, 145, 142, 151	184, 184, 181, 170	146, 141, 141
B(2,3,4)	5.81	174, 191, 175, 184	167, 145, 147, 155	146, 250, 146, 136	147, 138, 142
B(1,2,3,4)	7.82	146, 151, 146, 161	255, 140, 138, 144	163, 162, 152, 138	145, 139, 142
Ga(1)	0.39	183, 200, 179, 191	184, 174, 172, 182	186, 185, 180, 170	179, 172, 171
Ga(3)	0.17	174, 185, 173, 182	185, 174, 173, 182	200, 200, 186, 175	180, 171, 171
Ga(4)	−0.06	174, 185, 173, 182	185, 174, 173, 182	186, 186, 180, 170	188, 179, 179
Ga(1,2)	0.82	182, 198, 179, 191	198, 182, 179, 191	186, 186, 180, 170	178, 172, 172
Ga(2,3)	0.57	174, 184, 173, 182	200, 183, 180, 191	199, 200, 186, 176	179, 171, 172
Ga(2,4)	0.31	174, 184, 173, 181	200, 183, 180, 191	185, 186, 180, 170	187, 179, 177
Ga(3,4)	0.11	174, 185, 173, 182	185, 174, 173, 182	200, 200, 186, 175	188, 179, 179
Ga(1,2,3)	1.00	183, 198, 179, 191	198, 183, 179, 191	199, 199, 186, 176	178, 172, 172
Ga(1,2,4)	0.72	183, 198, 180, 191	198, 183, 180, 191	186, 186, 179, 170	186, 180, 180
Ga(2,3,4)	0.49	174, 184, 173, 181	200, 183, 181, 191	199, 200, 186, 175	187, 179, 181
Ga(1,2,3,4)	0.90	183, 198, 180, 190	198, 183, 180, 190	199, 199, 186, 176	186, 180, 180

[a]Corresponding to Figure 1(c).

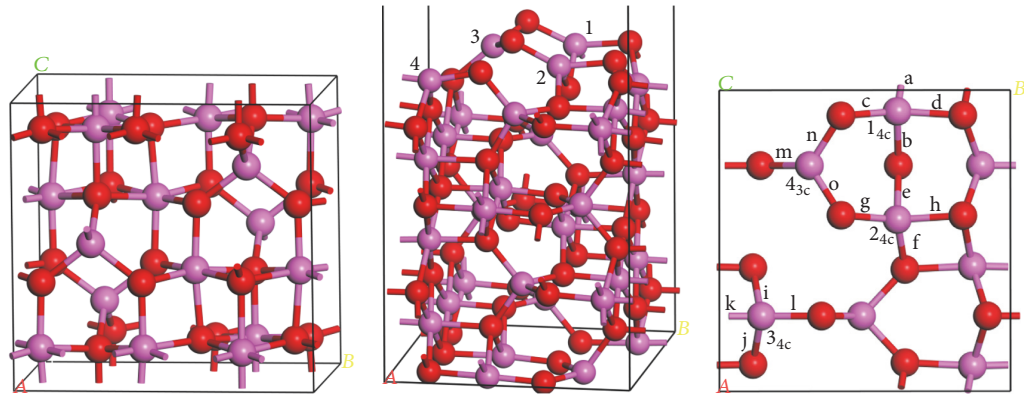

(a) (b) (c)

Figure 1: Side view of unit cell of γ-Al_2O_3 (a) and side (b) and top (c) views of the γ-Al_2O_3(110) surface (Al and O atoms are in rose and red, respectively. Coordination numbers of surface atoms are shown in subscript in (c)).

for Ga(3,4), Ga(1,2,4), and Ga(1,2,3,4). Since the Ga atom radius is larger than that of Al [35], the Ga–O bond distance is much longer than that of Al–O bond distance. In order to map out whether it is possible for B and Ga substitution for the bulk Al atoms of γ-alumina, we also calculated the substitution energies for the substitution of the sublayer hexa- and tetracoordinated Al atom by B and Ga atoms. The calculated substitution energies for B replacing the sublayer hexa- and tetracoordinated Al atoms are 4.34 and 2.89 eV, respectively, versus 0.81 and 0.57 eV for Ga, which are larger than the substitution energies for Al substitution on the surface. It indicates that the substitution reaction should favor happening on the surface, rather than in the bulk. In addition, the substitution of tetrahedral Al sites is always more thermodynamically favored than the substitution of octahedral Al sites.

As reported in the previous work [10], the substitution of γ-alumina surface Al by Fe atoms is thermodynamically favored, as the substitution energy for the substitution of all surfaces Al by Fe atom is −0.87 eV. It indicates that the Fe should be more easily to be incorporated into the γ-alumina than B and Ga.

3.2. Adsorption of Water Molecules on the X_2O_3 Surfaces (X = B, Al, Ga).* Figure 3 shows the structures and adsorption

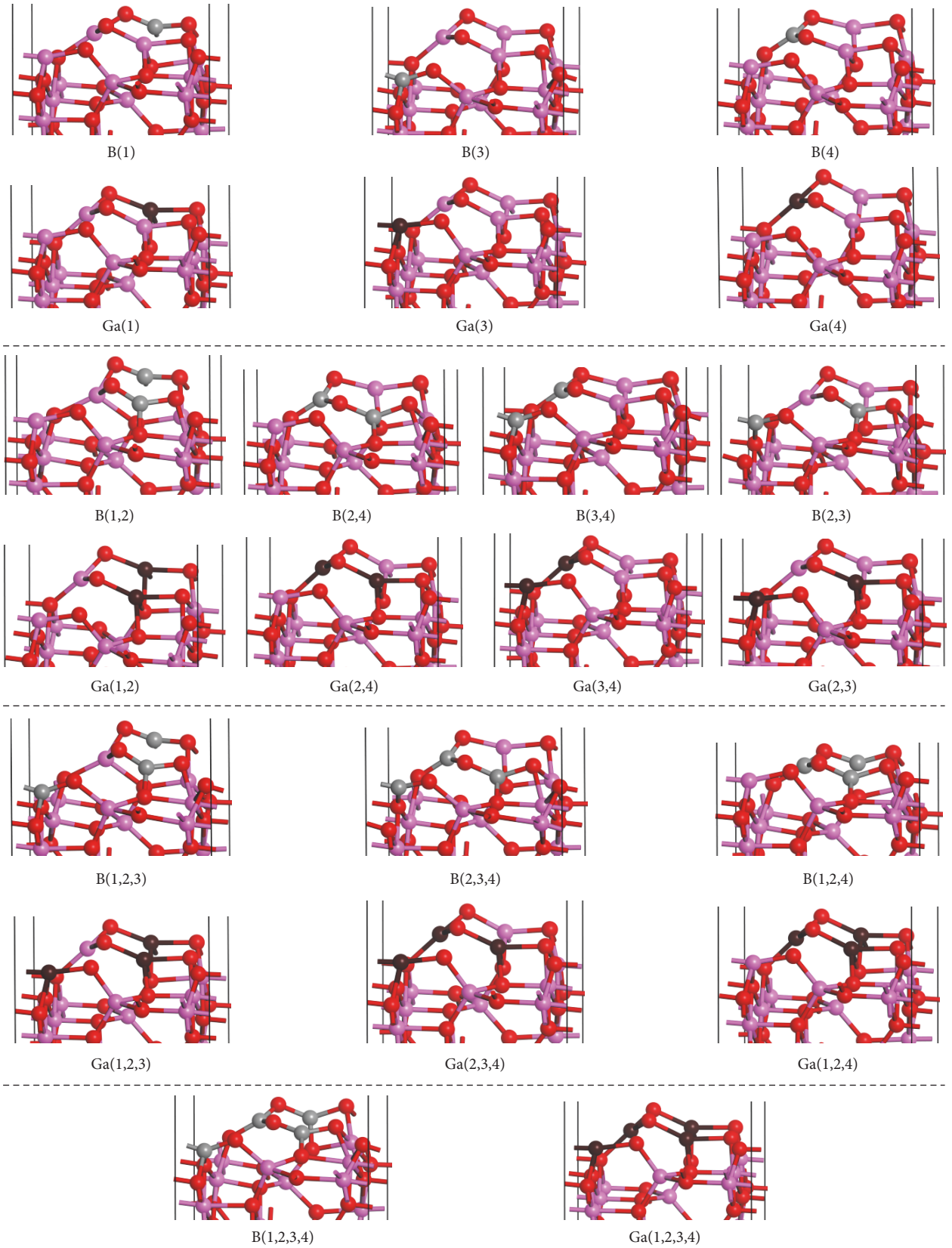

FIGURE 2: Side views of the B and Ga substituted γ-Al_2O_3(110) surface (B, Al, Ga, and O atoms are in gray, rose, dark, and red, resp.). All figures are indexed corresponding to Table 1.

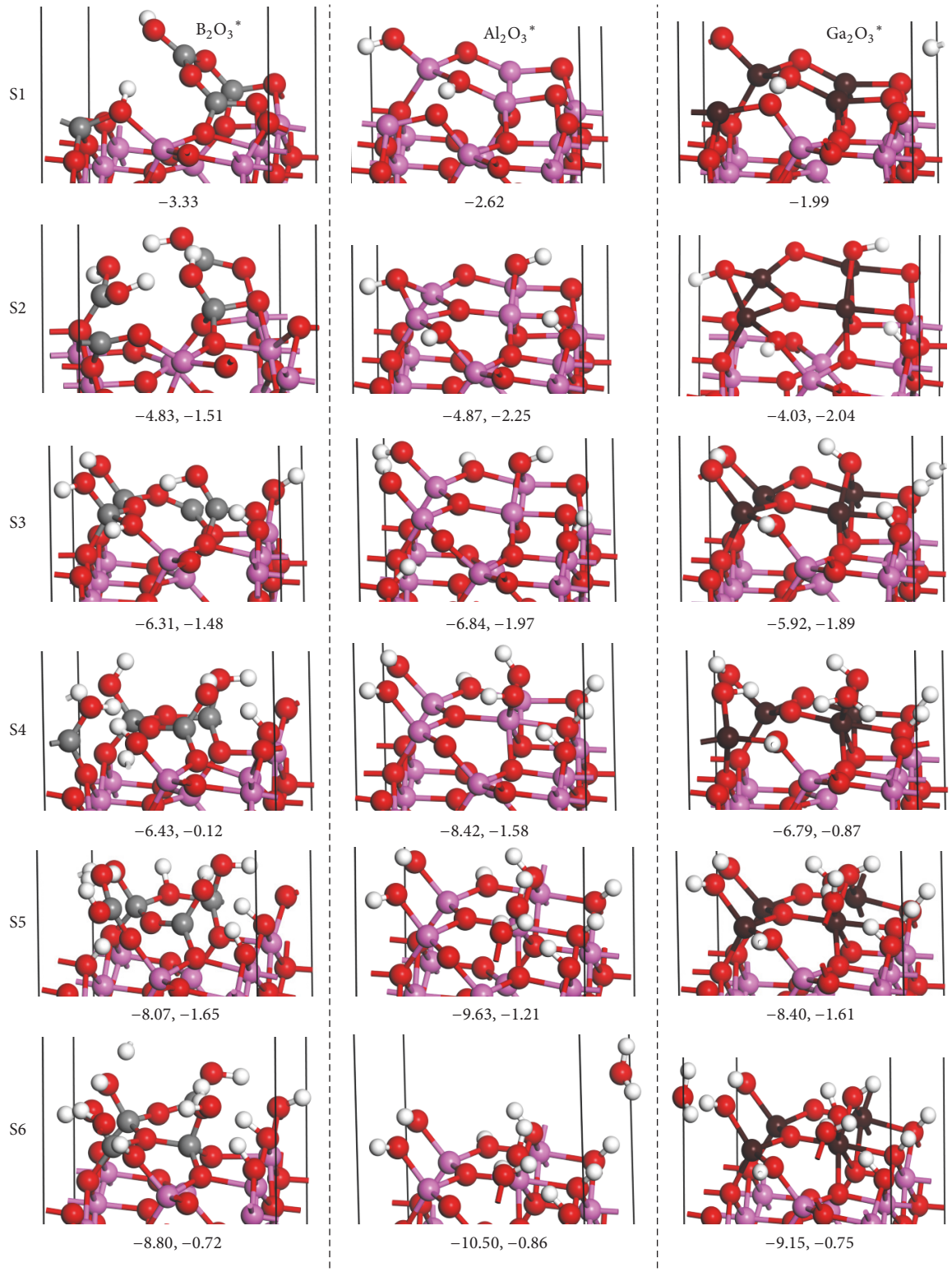

FIGURE 3: Side views for subsequent water adsorption on B_2O_3*, Al_2O_3*, and Ga_2O_3* surfaces, Sn (n = 1–6). The total and (subsequent) adsorption energies are given in eV. (B, Al, Ga, O, and H atoms are in gray, rose, dark, red, and white, resp.).

energies for water adsorption on the $B_2O_3^*$, $Al_2O_3^*$, and $Ga_2O_3^*$ surfaces. It should be noted that our calculated adsorption energies for the water adsorption on the $Al_2O_3^*$ surfaces are −2.62, −4.87, −6.84, −8.42, −9.63, and −10.50 eV, respectively, for 1–6 water molecules adsorbed on the γ-alumina surface. The stepwise adsorption energies for each water molecule are −2.62, −2.25, −1.97, −1.58, −1.21, and −0.86 eV. The previous works reported the adsorption of one water molecule on the γ-alumina (110) surface releases the energy of −2.49 eV [1, 32], which is slightly smaller than the results of present work (−2.62 eV). The reason is that the PBE-D3 methods were used in the present work and dispersion correction effects were taken into consideration. The optimized structures for the adsorption are the same as the previous works. The $Al_2O_3^*$ and $Ga_2O_3^*$ show similar structures with one −OH group on the tricoordinated surface Al/Ga atom, and H atom bonds to the twofold coordinated surface O atoms. It is interesting to see that the surface B–O bond was broken after water adsorption, and the âĂŠOH group from the water bonds to the surface BO_2 in coplanar. The H atom from the water adsorbs onto the surface of O atom forming an in-surface hydroxyl. It leads to a larger adsorption energy for the first water molecule adsorbed on the surface of $B_2O_3^*$ than that of $Al_2O_3^*$ and $Ga_2O_3^*$.

For two water molecules adsorption on the $B_2O_3^*$, $Al_2O_3^*$, and $Ga_2O_3^*$ surfaces, the adsorption energies are −4.83, −4.87, and −4.03 eV, respectively. $Al_2O_3^*$ shows the largest adsorption energy. The second water molecule makes the $B_2O_3^*$, $Al_2O_3^*$, and $Ga_2O_3^*$ surfaces seriously distorted. As shown in Figure 3, the X(3) atom moves to surface X(4) atom for X = Al and Ga, and they share one −OH group from the water and both became tetracoordinated.

As the water coverage increases from one to six water molecules in one $B_2O_3^*$ slab, the adsorption energy increases from −3.33, −4.83, −6.31, −6.43, and −8.07 to −8.80 eV, respectively. In comparison, the adsorption energy increases from −1.99, −4.03, −5.92, −6.79, and −8.40 to −9.15 eV for $Ga_2O_3^*$ surface. Both are smaller than those for the $Al_2O_3^*$ surface. It indicates that the pure γ-alumina surface shows stronger water adsorption than $B_2O_3^*$ and $Ga_2O_3^*$. It should be noted that the subsequent adsorption monotonously decreases for the water adsorption on $Al_2O_3^*$ surface. Since the water adsorption leads to the surface reconstruction, there are the turning points of the stepwise adsorption energy for 4-5 water molecules adsorption for the $B_2O_3^*$ and $Ga_2O_3^*$ slabs. In addition, the stepwise adsorption energy for the sixth water molecule adsorbent on the $B_2O_3^*$, $Al_2O_3^*$, and $Ga_2O_3^*$ surfaces is similar (−0.72, −0.86, and −0.75 eV, resp.). The main reason is that the former five water molecules have totally covered the active sites for water adsorption, and the sixth water molecule could only be physically adsorbed.

4. Conclusions

The dispersion corrected periodic density functional theory was used to investigate the structure and energies for the B and Ga incorporated γ-alumina surface. The results show that the substitution of Al by B is not thermodynamically favored on the surface. However, the substitution of Al by Ga is thermodynamically favored at low coverage on the surface. The substitution reaction prefers to occur at the tricoordinated A(4) sites. The substitution reaction becomes thermodynamically not favored as more and more B and Ga substitutions take place on the surface. The substitutions of Al by B and Ga are not so favored in the bulk as that for the surface.

The adsorption of water molecules on the B and Ga incorporated γ-alumina surface was also investigated and compared to that of the pure γ-alumina surface. It shows that the γ-alumina surface has the strongest adsorption ability for water adsorption. The total adsorption energy increases as water coverage increases from one to six water molecules in each slab, while the stepwise adsorption energy decreases. On the $B_2O_3^*$, $Al_2O_3^*$, and $Ga_2O_3^*$ surfaces, the sixth could only be physically adsorbed on the surface, since the former adsorbed five water molecules (at the coverage of 7.5 H_2O/nm^2) fully covered the active sites for water adsorption.

Conflicts of Interest

The authors declare that there are no conflicts of interest regarding the publication of this paper.

Acknowledgments

This work was supported by the Doctoral Scientific Research Foundation for Dr. Lihong Cheng of Jiangxi Science & Technology Normal University (2017.1-2020.12), Science Foundation of Jiangxi Department of Education (GJJ150827), and National Natural Science Foundation of Jiangxi Province (20151BAB204009).

References

[1] G. Feng, C.-F. Huo, C.-M. Deng et al., "Isopropanol adsorption on γ-Al_2O_3 surfaces: a computational study," *Journal of Molecular Catalysis A: Chemical*, vol. 304, no. 1-2, pp. 58–64, 2009.

[2] L. Huang, Y.-L. Zhu, C.-F. Huo et al., "Mechanistic insight into the heterogeneous catalytic transfer hydrogenation over Cu/Al_2O_3: direct evidence for the assistant role of support," *Journal of Molecular Catalysis A: Chemical*, vol. 288, no. 1-2, pp. 109–115, 2008.

[3] Y. Liu, J. Liu, G. Feng, S. Yin, W. Cen, and Y. Liu, "Interface effects for the hydrogenation of CO_2 on Pt_4/γ-Al_2O_3," *Applied Surface Science*, vol. 386, pp. 196–201, 2016.

[4] B. Ealet, M. H. Elyakhloufi, E. Gillet, and M. Ricci, "Electronic and crystallographic structure of γ-alumina thin films," *Thin Solid Films*, vol. 250, no. 1-2, pp. 92–100, 1994.

[5] J. Libuda, F. Winkelmann, M. Bäumer et al., "Structure and defects of an ordered alumina film on NiAl(110)," *Surface Science*, vol. 318, no. 1-2, pp. 61–73, 1994.

[6] D. W. Susnitzky and C. B. Carter, "The formation of copper aluminate by solid-state reaction," *Journal of Materials Research*, vol. 6, no. 9, pp. 1958–1963, 1991.

[7] G. A. El-Shobaky, N. M. Ghoneim, and E. A. Sultan, "Thermal decomposition of nickel aluminium mixed hydroxides and formation of nickel aluminate spinel," *Thermochimica Acta*, vol. 63, no. 1, pp. 39–49, 1983.

[8] T. Wang, F. Jiang, G. Liu, L. Zeng, Z.-J. Zhao, and J. Gong, "Effects of Ga doping on Pt/CeO_2-Al_2O_3 catalysts for propane dehydrogenation," *AIChE Journal*, vol. 62, no. 12, pp. 4365–4376, 2016.

[9] B. Bonnetot, V. Rakic, T. Yuzhakova et al., "Preparation and characterization of Me_2O_3-CeO_2 (Me = B, Al, Ga, In) mixed oxide catalysts. 2. Preparation by sol-gel method," *Chemistry of Materials*, vol. 20, no. 4, pp. 1585–1596, 2008.

[10] G. Feng, C.-F. Huo, Y.-W. Li, J. Wang, and H. Jiao, "Structures and energies of iron promoted γ-Al_2O_3 surface: a computational study," *Chemical Physics Letters*, vol. 510, no. 4–6, pp. 224–227, 2011.

[11] H.-J. Wan, B.-S. Wu, C.-H. Zhang et al., "Study on Fe-Al_2O_3 interaction over precipitated iron catalyst for Fischer-Tropsch synthesis," *Catalysis Communications*, vol. 8, no. 10, pp. 1538–1545, 2007.

[12] V. G. De Resende, X. Hui, C. Laurent, A. Weibel, E. De Grave, and A. Peigney, "Fe-substituted mullite powders for the in situ synthesis of carbon nanotubes by catalytic chemical vapor deposition," *Journal of Physical Chemistry C*, vol. 113, no. 26, pp. 11239–11245, 2009.

[13] V. G. de Resende, A. Cordier, E. De Grave et al., "Synthesis of γ-$(Al_{1-x}Fe_x)_2O_3$ solid solutions from oxinate precursors and formation of carbon nanotubes from the solid solutions using methane or ethylene as carbon source," *Journal of Materials Research*, vol. 23, no. 11, pp. 3096–3111, 2008.

[14] V. G. de Resende, A. Cordier, E. de Grave et al., "Presence of metallic Fe nanoclusters in α-$(Al,Fe)_2O_3$ solid solutions," *The Journal of Physical Chemistry C*, vol. 112, no. 42, pp. 16256–16263, 2008.

[15] G. Feng, D. Yang, D. Kong, J. Liu, and Z.-H. Lu, "A comparative computational study on the synthesis prescriptions, structures and acid properties of B-, Al- and G-incorporated MTW-type zeolites," *RSC Advances*, vol. 4, no. 89, pp. 47906–47920, 2014.

[16] J. Zhou, J. Teng, L. Ren et al., "Full-crystalline hierarchical monolithic ZSM-5 zeolites as superiorly active and long-lived practical catalysts in methanol-to-hydrocarbons reaction," *Journal of Catalysis*, vol. 340, pp. 166–176, 2016.

[17] C. G. Zuo, A. G. Xiao, Z. H. Zhou et al., "Spectroscopic properties of Ce^{3+}-doped $BaO–Gd_2O_3–Al_2O_3–B_2O_3–SiO_2$ glasses," *Journal of Non-Crystalline Solids*, vol. 452, pp. 35–39, 2016.

[18] V. A. Silva, P. C. Morais, R. F. Morais, and N. O. Dantas, "Successful Nd^{3+} doping of $Li_2O–B_2O_3–Al_2O_3$ vitreous system: optical characterization and judd–ofelt spectroscopic calculations," *Brazilian Journal of Physics*, vol. 46, no. 6, pp. 643–648, 2016.

[19] J. L. Jansons, P. A. Kulis, Z. A. Rachko et al., "Luminescence of Ga-doped alpha-Al_2O_3 crystals," *Physica Status Solidi B-Basic Research*, vol. 120, no. 2, pp. 511–518, 1983.

[20] M. E. Kibar, O. Özcan, Y. Dusova-Teke, E. Yonel-Gumruk, and A. N. Akin, "Optimization, modeling and characterization of sol-gel process parameters for the synthesis of nanostructured boron doped alumina catalyst supports," *Microporous and Mesoporous Materials*, vol. 229, pp. 134–144, 2016.

[21] J. P. Perdew, K. Burke, and M. Ernzerhof, "Generalized gradient approximation made simple," *Physical Review Letters*, vol. 77, no. 18, pp. 3865–3868, 1996.

[22] G. Kresse and J. Furthmüller, "Efficiency of ab-initio total energy calculations for metals and semiconductors using a plane-wave basis set," *Computational Materials Science*, vol. 6, no. 1, pp. 15–50, 1996.

[23] G. Kresse and J. Furthmüller, "Efficient iterative schemes for ab initio total-energy calculations using a plane-wave basis set," *Physical Review B - Condensed Matter and Materials Physics*, vol. 54, no. 16, pp. 11169–11186, 1996.

[24] J. Liu, Z.-F. Liu, G. Feng, and D. Kong, "Dimerization of propene catalyzed by Brønsted acid sites inside the main channel of zeolite SAPO-5: a computational study," *The Journal of Physical Chemistry C*, vol. 118, no. 32, pp. 18496–18504, 2014.

[25] G. Feng, Y.-Y. Lian, D. Yang, J. Liu, and D. Kong, "Distribution of Al and adsorption of NH_3 and pyridine in ZSM-12: a computational study," *Canadian Journal of Chemistry*, vol. 91, no. 10, pp. 925–934, 2013.

[26] S. Grimme, A. Hansen, J. G. Brandenburg, and C. Bannwarth, "Dispersion-corrected mean-field electronic structure methods," *Chemical Reviews*, vol. 116, no. 9, pp. 5105–5154, 2016.

[27] S. Grimme, S. Ehrlich, and L. Goerigk, "Effect of the damping function in dispersion corrected density functional theory," *Journal of Computational Chemistry*, vol. 32, no. 7, pp. 1456–1465, 2011.

[28] S. Grimme, J. Antony, S. Ehrlich, and H. Krieg, "A consistent and accurate ab initio parametrization of density functional dispersion correction (DFT-D) for the 94 elements H-Pu," *Journal of Chemical Physics*, vol. 132, no. 15, Article ID 154104, 2010.

[29] G. Kresse and D. Joubert, "From ultrasoft pseudopotentials to the projector augmented-wave method," *Physical Review B*, vol. 59, no. 3, pp. 1758–1775, 1999.

[30] P. E. Blöchl, C. J. Först, and J. Schimpl, "Projector augmented wave method: ab initio molecular dynamics with full wave functions," *Bulletin of Materials Science*, vol. 26, no. 1, pp. 33–41, 2003.

[31] P. E. Blöchl, "Projector augmented-wave method," *Physical Review B*, vol. 50, no. 24, pp. 17953–17979, 1994.

[32] M. Digne, P. Sautet, P. Raybaud, P. Euzen, and H. Toulhoat, "Use of DFT to achieve a rational understanding of acid-basic properties of γ-alumina surfaces," *Journal of Catalysis*, vol. 226, no. 1, pp. 54–68, 2004.

[33] J. Wang, H. Yu, L. Geng et al., "DFT Study of Hg Adsorption on M-substituted Pd(111) and PdM/γ-Al_2O_3(110) (M = Au, Ag, Cu) Surfaces," *Applied Surface Science*, vol. 355, pp. 902–911, 2015.

[34] L. Geng, L. Han, W. Cen et al., "A first-principles study of Hg adsorption on Pd(111) and Pd/γ-Al_2O_3(110) surfaces," *Applied Surface Science*, vol. 321, pp. 30–37, 2014.

[35] B. Cordero, V. Gómez, A. E. Platero-Prats et al., "Covalent radii revisited," *Dalton Transactions*, no. 21, pp. 2832–2838, 2008.